

## Shear-Induced Diffusion in Dilute Suspensions of Charged Colloids

Victor Breedveld<sup>#</sup> and Alex J. Levine<sup>\*</sup>

<sup>1</sup>Department of Chemical Engineering and Materials Research Laboratory, University of California at Santa Barbara, Santa Barbara, California, USA

### ABSTRACT

We propose a model for the nonequilibrium enhancement of colloidal self-diffusion in an externally imposed shear flow in charged systems. The diffusion enhancement is calculated in terms of electrostatic, two-body interactions between the particles in shear flow. In the high-shear rate, low-volume fraction limit in which the model is valid, we compare these calculations to the experiments of Qiu et al. [PRL 61, 2554 (1988)] and simulations of Chakrabarti et al. [PRE 50, R3326 (1994)] and find good agreement on scaling and magnitude to within experimental uncertainty of the electrostatic parameters.

*Key Words:* PACS numbers; 47.15.Pn; 51.20+d; 83.80Hj.

---

<sup>#</sup>Current address: Victor Breedveld, School of Chemical Engineering, Georgia Institute of Technology, Atlanta, GA, USA.

<sup>\*</sup>Correspondence: Alex J. Levine, Department of Physics, University of Massachusetts at Amherst, Amherst, MA 01003, USA; E-mail: levine@physics.umass.edu.



## INTRODUCTION

In addition to their practical importance for and ubiquity in industrial processing, colloidal suspensions<sup>[1,2]</sup> serve as a unique model system with which to study the equilibrium properties of atomic liquids and solids due to their inherently longer lengths and time scales. In addition, these longer lengths and time scales of colloid systems offer the opportunity to experimentally probe fundamental issues regarding many-body, nonequilibrium dynamics in strongly interacting (*charged*) systems. The long relaxation times of the system allow it to be driven far from equilibrium through, e.g., the application of moderate shear rates. Such issues remain among the principal puzzles of modern statistical mechanics and can thus be explored experimentally through colloids. For the theorist interested in nonequilibrium statistical physics, the exploration of colloidal systems promises one of the most direct connections to experiment.

In this paper, we discuss the origin of an intriguing and apparently generic feature of particulate suspensions driven out of equilibrium by the application of shear flow. Since its initial observation by Qiu et al.<sup>[3]</sup> in a charged colloidal suspension, it is now well known that the effective single-particle diffusion constant grows under shear. Similar enhancement of self-diffusion under applied shear has been observed in concentrated noncolloidal (i.e., non-Brownian or high Peclet number) suspensions, experimentally<sup>[4,5]</sup> and in simulations.<sup>[6]</sup> It should be pointed out that this diffusion enhancement occurs in the gradient and vorticity directions, and is thus unrelated to the better-understood Taylor dispersion that contributes to the effective diffusion along the flow direction.

In approaching this problem, we note a general point: two-body interactions in the suspension that obey time-reversal symmetry cannot be the cause of a mechanism for diffusion. Because laminar, zero Reynolds number flow is symmetrical under time reversal, one is forced to look elsewhere to understand nonequilibrium diffusion enhancement. In uncharged, noncolloidal suspensions, it has been shown numerically that three-particle hydro-dynamic interactions are chaotic.<sup>[7,8]</sup> These chaotic interactions were previously implicated as a source of nonthermal noise in nonequilibrium suspensions.<sup>[9]</sup> In addition, finite particle roughness<sup>[10]</sup> can break the symmetry of low Reynolds number hydrodynamics effectively, by cutting off lubrication forces at small interparticle separations.

In charged colloidal systems, there is, however, another source of symmetry breaking due to the electrostatic interactions between the colloids<sup>[2,11,12]</sup> (see Figure 1). The long-range electrostatic repulsion between colloidal particles has a number of well-known effects on the equilibrium structure of colloidal suspensions. For example, this interparticle repulsion drives the colloidal system into an ordered solid phase at volume

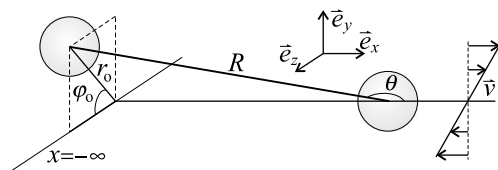


**Figure 1.** Coordinate system for two-particle collision in a shear flow with the right particle as the origin of the reference frame.

fractions well below the liquid-to-crystal transition on the hard-sphere phase diagram. These electrostatic interactions clearly have an impact on the out of equilibrium dynamics of the system as well. Their importance in the diffusion enhancement observed by Qiu et al. is demonstrated by the fact that a decrease in the Debye screening length suppresses the effect. Based on this observation, we build our theory for diffusion enhancement in the nonequilibrium suspension upon the electrostatic breaking of time reversal symmetry of particle trajectories within the shear flow. Fortunately, these electrostatic perturbations to the particle trajectories are more analytically tractable than the chaotic, many-body hydrodynamics that presumably generates a similar diffusion enhancement in non-Brownian hard-sphere suspensions. We suspect, however, that such chaotic effects, which play a role only when three or more particles pass within a few particle radii, become increasingly important for randomization of particle trajectories at higher-volume fractions. On the other hand, the electrostatic effects that we analyze in this paper, presumably dominate the diffusion enhancement at low-volume fractions.

The remainder of the paper is organized as follows: in the next section, we develop the fundamental trajectory calculation for two electrostatically interacting colloids passing each other in the externally imposed, uniform shear flow. We then explore the consequences of this trajectory calculation for the enhancement of diffusion, which we report in the following section. We conclude in this section by further discussing these results and comparing them in quantitative detail to experiment and simulation.

## THEORY

Our calculation proceeds as follows: In a collection of particles of radius  $a$  at volume fraction  $\phi$ , we consider the randomization of the trajectory of a particle, which we refer to as the scattering center, due to its electrostatic interaction with a collection of identical particles that are carried past it in the shear flow. This is done in two steps. We first compute the trajectory of a charged colloid as the macroscopic shear flow (uniform shear rate  $\dot{\gamma}$ ) carries it past the scattering center; from this calculation, we determine the displacement of the scattering center. Given a spatially random ensemble of the incoming particles, we compute the second moment of the displacements of the scattering center due to interactions with the particles flowing past it. The product of this second moment with the rate of scattering events ( $\sim \dot{\gamma}$ ) gives the shear enhancement of the diffusion constant  $\Delta D \sim |\dot{\gamma}|^\alpha$ . We compare the magnitude of this diffusion enhancement and its dependence upon shear rate (i.e.,  $\alpha$ ) by experiment.

Qualitatively, the trajectory of a charged particle under the combined influence of macroscopic shear flow and electrostatic interaction with the scattering center can be described as follows. The shear flow brings a particle toward the scattering center along a given stream line. While the particle resides within a few screening lengths of the scattering center, the electrostatic interaction displaces the particle from its stream line. However, once the particle has been carried by the combination of flow and electrostatic interaction to a distance of more than a few screening lengths, the particle resumes its trajectory along a different streamline than the one on which it entered. See Figure 2 for computed trajectories.

There are two simple, heuristic limits resulting from the dominance of one of two independent forces controlling the particle trajectories, hydrodynamic drag and the interparticle, electrostatic interaction. These limits result in qualitatively different



particle trajectories and a different dependence of diffusion enhancement upon shear rate. It must be emphasized that the experimentally studied case, which is the focus of this paper, lies intermediate to these two limits.

In the case of an arbitrarily strong electrostatic interaction, this force completely controls the motion of a particle in the interaction zone, and we recover a simple linear dependence of the diffusion enhancement upon shear. A particle enters the interaction zone along some stream line. Now, the dominant electrostatic repulsion between that particle and the scattering center drives the particle out of the interaction zone. It then resumes its straight-line motion along a different stream line. The displacement of the particle is thus on the order of the interaction zone radius and is independent of the imposed shear rate. The scattering rate, however, is proportional to the shear rate, so that the diffusion enhancement scales linearly with shear rate,  $\Delta D \sim |\dot{\gamma}|$  in the low-shear rate regime, where the particle-particle interaction is entirely dominated by the electrostatics (Figure 2a).

On the other hand, if the electrostatic interaction is weak enough, or, equivalently, if the shear rate is high enough, a particle will be carried predominantly by the shear flow through the electrostatic interaction zone surrounding the scattering center. In this case, the residence time of the particle in the interaction zone is inversely proportional to the shear rate. In the low Reynolds number limit (which we

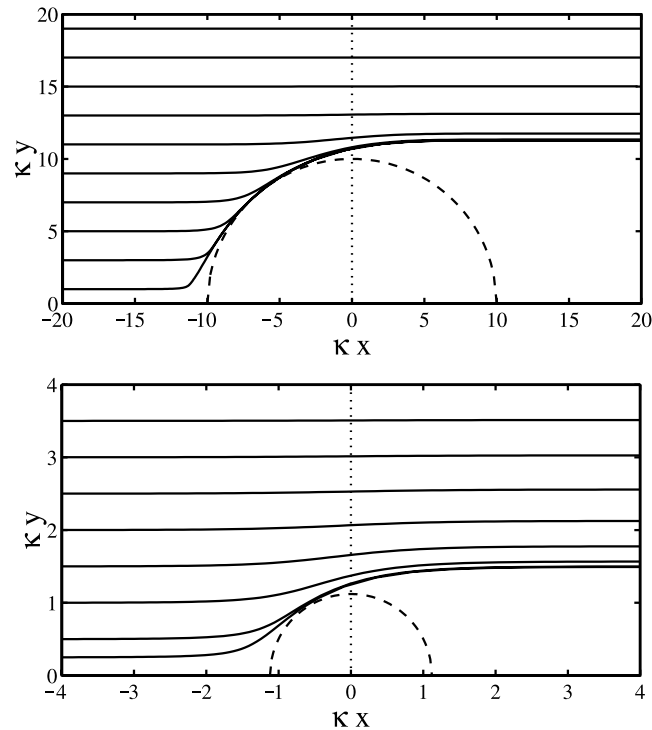


**Figure 2.** Trajectories in the  $x$ - $y$  plane (i.e.,  $\varphi_0 = \pi/2$ ) for the collision between two electrostatically interacting colloids in a shear flow;  $H = 10^6$  in the upper figure, and  $H = 1$  in the lower figure; trajectories are plotted for different impact parameters  $\hat{h}_0$ . The dashed semicircles denote the volume of the interaction zone surrounding the scattering center.

always assume), the displacement of the particle from its initial stream line is proportional to the time integral of the force acting on it. In this case, that time integral will be proportional to  $\dot{\gamma}^{-1}$ . Because the rate of scattering events will still be proportional to  $\dot{\gamma}$ , we expect that the enhancement of diffusion will plateau at high-shear rates (Figure 2b).

The cases described above represent only the limiting cases of strong and weak shear. Not surprisingly, for physical values of the ratio of the two forces, including those encountered in experiment, the predicted result for shear enhancement interpolates between these limits. We find for a broad range of shear rates and for physically relevant electrostatic interaction parameters that the shear enhancement of diffusion scales is  $\Delta D \sim |\dot{\gamma}|^{0.7}$ .

Our calculation cannot be extended to zero  $\dot{\gamma}$ . We estimate a lower shear-rate cutoff for our analysis by noting that we assume that particles follow stream-lines toward and away from the scattering center, except when they are within the interaction zone surrounding each particle. If the shear rate is so low that particles can exhibit significant diffusion while moving through the interaction zone, the deterministic trajectory calculations are no longer valid. The crossover from our model calculations to quadratic scaling occurs at a critical shear rate  $\dot{\gamma}^* \sim \kappa^2 D_0$ , where  $D_0$  is the Brownian diffusion constant. At this crossover shear rate, a particle diffuses a Debye length in the same time as it is advected that distance by the flow. For the experimental system in question,  $\dot{\gamma}^* = 10^2 \text{ s}^{-1}$ . In addition, we note that the reduction of many-body interactions into a series of simple two-body interactions can only be justified in the limit of small particle number density.

The resulting scaling of the shear enhancement of diffusion with shear rate is in good agreement with nonequilibrium, Brownian-dynamics simulations.<sup>[13,14]</sup> The experimental data,<sup>[3]</sup> however, suggest a power law of unity. To resolve this discrepancy, we point out that our calculation is not applicable to the lower shear rate experimental data. In this lower shear rate regime, we expect that the shear-rate dependence of  $\Delta D$  is stronger than linear,<sup>[16]</sup> so that the effect of the crossover of the exponent from greater than one to 0.7 leads to a larger apparent exponent in the data.<sup>a</sup> Second, we note that over the single decade of shear-rate data available, it is problematic to distinguish between our proposed exponent of 0.7 and the linear dependence on shear rate concluded by Qiu et al. In addition, we will show that by making reasonable assumptions about the electrostatic interactions present in the experimental system of Qiu et al., our calculation of the magnitude of the shear enhancement effect agrees well with the experiment.

In an earlier mode-coupling study, Indrani et al.<sup>[15]</sup> attribute the diffusion enhancement to the suppression of the effective friction,  $\zeta$ , experienced by a concentration fluctuation. Noting that  $D \sim T/\zeta$ , they calculate the contribution to  $\zeta$  from the interaction of a particle concentration fluctuation with all other thermally generated concentration fluctuations in the medium. The principal effect of the shear flow is to destroy these concentration fluctuations and, thereby, decrease the effective friction. We, on the other hand, propose that the principal effect of the shear flow when considered along with the electrostatic interparticle interactions is to increase the effective temperature in the nonequilibrium system.

<sup>a</sup>We note that similar arguments were made in Ref. [15].



The particle trajectories are described by the following differential equation:<sup>[17]</sup>

$$\frac{dY}{d\xi} = Y \frac{\xi}{1 + \xi^2} + \frac{H}{\sin \varphi} \frac{Y + 1}{Y^2} e^{-Y} \quad (1)$$

where  $Y = \kappa R$  is the distance of the incoming particle from the scattering center measured in Debye lengths  $\kappa^{-1}$ , and  $\xi = \cot \theta$  is the polar angle (Figure 1). Eq. 1 accounts for the interplay of the hydrodynamic drag force by the fluid represented by the first term and electrostatic repulsion between particles represented by second term on the RHS of Eq. 1. The relative importance of these two forces is measured by the dimensionless parameter  $H$ , which represents the ratio between the electrostatic interparticle interaction and the hydrodynamic drag.  $H$  is defined by

$$H = \frac{8\pi\epsilon_r\epsilon_0\Phi_a^2(\kappa a)^2 e^{2\kappa a}\kappa}{\zeta\dot{\gamma}} = \frac{C}{\dot{\gamma}} \quad (2)$$

where  $\epsilon_r\epsilon_0$  is the dielectric constant of the fluid,  $\Phi_a$  the apparent surface potential of the particles, and  $\zeta$  the hydrodynamic friction factor. All the details of the electrostatic interaction for a given colloidal system can be subsumed into the parameter  $C$  defined above.

Eq. 1 neglects hydrodynamic interactions between particles, which is acceptable if particles, do not make close passes. In a dilute suspension of highly charged colloids, the number of such close passes should be negligible and thus not greatly contribute to the effective diffusion constant. This view is supported by the original experiments that showed that the shear enhancement of diffusion disappears with sufficient screening of the electrostatic interaction.<sup>[3]</sup>

To determine the trajectory of a scattering particle, we integrate Eq. 1 from initial conditions such that at large distances from the scattering center (i.e.,  $x \rightarrow -\infty$ ), the incoming particle has an impact parameter  $r_0$  and a polar angle  $\varphi_0$  measured from the axis in the  $yz$  plane. Due to the central nature of the electrostatic forces, every trajectory is confined to a plane of constant  $\varphi$ . However, because  $\hat{y}$  is the velocity gradient direction of the imposed shear flow, the rate of incoming particles to the scattering center will depend on  $\varphi$ . We show in Figure 2 two sets of numerically integrated trajectories. The first set represents the electrostatically dominated regime (high  $H$ ), and the second set shows the shear flow dominated regime (low  $H$ ).

We determine the total displacement of the incoming particle normal to the stream lines by finding the change in the radial distance  $\Delta\hat{r} = \kappa(r|_{x \rightarrow \infty} - r_0)$  of the particle's trajectory to the  $\hat{x}$  axis, comparing the asymptotic out-state, where  $x \rightarrow \infty$  to the initial impact parameter. By symmetry, each particle (the incoming particle and the scattering center) moves half of the distance  $\Delta\hat{r}$  in the laboratory frame.

For collisions between two interacting colloids with initial conditions in the  $x$ - $y$  plane ( $\varphi_0 = \pi/2$ , see Figure 2 for trajectories), the displacement  $\Delta\hat{r}$  is plotted as a function of the impact parameter  $\hat{r}_0 = \kappa r_0$  and the dimensionless interaction parameter  $H$  in Figure 3. Because the motion is restricted to the  $x$ - $y$  plane,  $\Delta\hat{r}$  is equivalent to  $\kappa \Delta y$ . The upper graph of Figure 3 clearly illustrates that the significant particle interactions take place only in a well-defined range of impact parameters, the scattering zone. If particle pairs start their collision inside this interaction zone, they undergo significant displacements; otherwise, they move along virtually undisturbed. The scattering zone expands with increasing values of  $H$ , as might be expected. In the lower

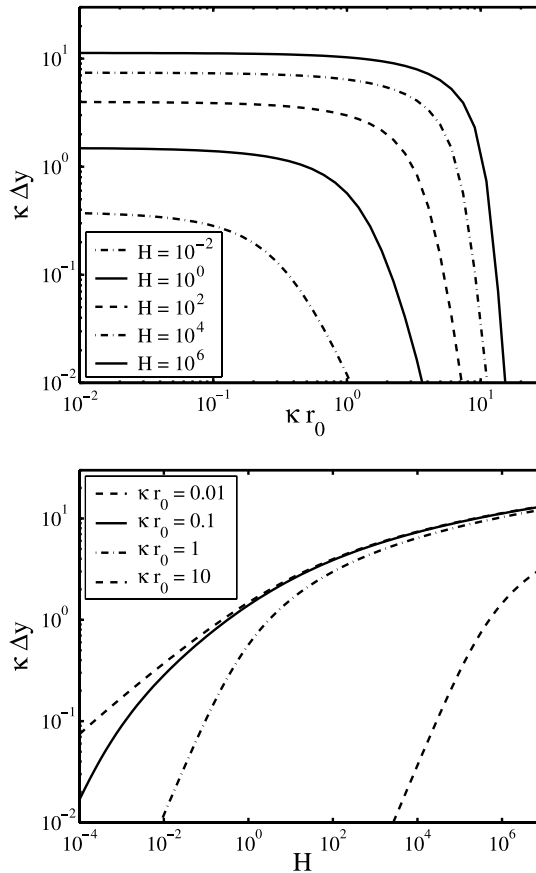


**Figure 3.** Dimensionless displacements  $\kappa \Delta y$  for colliding particle pairs with trajectories in the  $x$ - $y$  plane ( $\phi_0 = \pi/2$ ); the upper graph presents  $\kappa \Delta y$  as a function of dimensionless impact parameter  $\kappa r_0$ , while the lower graph illustrates the dependence of  $\kappa \Delta y$  on the interaction parameter  $H$ .

graph of Figure 3, one can see what happens if  $\hat{r}_0$  is kept constant while the electrostatic interaction becomes stronger with respect to flow (increasing  $H$ ). The displacements are increasing as well, in a nontrivial way. For every impact parameter, the displacements initially grow rapidly with  $H$  and then level off for flow conditions dominated by electrostatics (high  $H$ ).

Presented in Figures 2 and 3 are the particle displacements for one initial orientation of the colliding pair ( $\phi_0 = \pi/2$ ). In order to calculate diffusion coefficients, all possible orientations need to be considered.

The effective enhancement of the diffusion constant in the velocity gradient ( $y$ ) and vorticity ( $z$ ) directions can be calculated from the second moment of the particle displacements in the appropriate directions:

$$\Delta D_{yy} = \frac{1}{2} \kappa^{-2} \int P(s) \left( \frac{1}{2} \Delta \hat{r}(s) \sin \phi_0 \right)^2 d^2 s \tag{3}$$



$$\Delta D_{zz} = \frac{1}{2} \kappa^{-2} \int P(s) \left( \frac{1}{2} \Delta \hat{r}(s) \cos \varphi_0 \right)^2 d^2 s \quad (4)$$

where  $P(s) ds$  is the probability per unit time of a collision to occur with impact parameter  $s = (\hat{r}_0, \varphi_0)$ , where  $\hat{r}_0 = \kappa r_0$  is made dimensionless. The terms in parentheses represent the displacements of a given particle in the respective directions. Assuming a random distribution of particles,  $P(s)$  is given by the particle flux through the area  $r_0 dr_0 d\varphi_0$ :

$$P(s) d^2 s = \frac{3\phi}{4\pi(\kappa a)^3} \dot{\gamma} \sin \varphi_0 \hat{r}_0^2 d\hat{r}_0 d\varphi_0 \quad (5)$$

The integration domain in Eqs. 3 and 4 only accounts for particles flowing in from the left ( $y > 0$ ). The diffusion constants are doubled to account for the contribution of the particle flux from the right ( $y < 0$ ). As expected, the shear rate  $\dot{\gamma}$  affects shear-enhanced diffusion in two distinct ways: through the particle flux ( $\sim \dot{\gamma}$ ) and the step size, which depends on  $H = C/\dot{\gamma}$  in a complicated way that we explore below.

## RESULTS AND DISCUSSION

To explore the shear rate dependence, it is convenient to express the diffusion constants in the following form, combining Eqs. 2, 3, and 4:

$$\Delta D_{\alpha\alpha} = \frac{3\phi}{4\pi(a\kappa)^3 \kappa^2} \frac{C}{H} I_\alpha(H) \quad (6)$$

where  $I_\alpha$  is a dimensionless integral ( $\alpha = y, z$ ). The entire shear rate dependence is now contained in  $1/H \cdot I_\alpha(H)$ , where  $H \sim 1/\dot{\gamma}$ . Figure 4 are shown in the results of our calculations in this dimensionless form:  $1/H \cdot I_\alpha(H) \sim \Delta D_{\alpha\alpha}$  vs.  $1/H \sim \dot{\gamma}$ .

For small values of  $H$  (large  $\dot{\gamma}$  or low interaction), the  $H$  dependence of  $I_\alpha(H)$  is linear, as can be seen by simple perturbation theory in  $H$ .  $\Delta D_{\alpha\alpha}$  at these large shear rates becomes independent of  $H$ . For large  $H$ , however, the dependence on  $H$  weakens, and the curves are described well by  $I_\alpha(H) \sim H^{0.3}$ , so that the diffusion enhancement, which scales as  $1/H \cdot I_\alpha(H)$ , takes the form:  $\Delta D_{\alpha\alpha} \sim 1/H \cdot I_\alpha(H) \sim H^{-0.7} \sim \dot{\gamma}^{0.7}$ . At small shear rates, the diffusion enhancement is anisotropic,  $\Delta D_{yy} / \Delta D_{zz} \approx 1.7$ , which is a geometrical effect related to the shear flow.

That the power law scaling holds over a wide range of shear rates is one of the central results of this paper. The power law of 0.7 is not inconsistent with the experimental data of Qiu et al., because it is difficult to distinguish from an exponent of unity over the limited range of the experimental shear rates where we expect our model to be valid ( $> 100 \text{ s}^{-1}$ ). In addition, the computed exponent agrees well with previous simulations of the system.<sup>[14]</sup> The scaling of the diffusivity with shear rate is distinctly different from that observed in noncolloidal suspensions, where shear-induced diffusion grows linearly with  $\dot{\gamma}$ .

In addition to the scaling, the calculations make testable predictions about the magnitude of  $\Delta D$ . To test this point, we need to obtain a value for  $C$  that depends on the surface potential of the colloids  $\Phi_a$ , the Debye screening length  $\kappa^{-1}$ , the particle



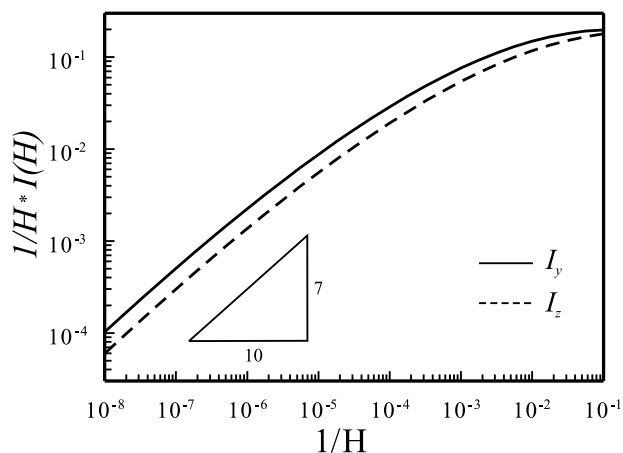


**Figure 4.** Scaling of diffusion with shear rate represented by the equivalent plot of  $I(H)/H$  vs.  $1/H$ .

radius  $a$ , and the effective particle mobility  $\zeta^{-1}$ . We determined the sphere mobility empirically from single-particle diffusion in the uncharged system, and, thus, only need the electrostatic parameters to determine  $C$  and calculate the diffusivity enhancement under shear. The model does not contain adjustable parameters beyond these physical quantities.

Unfortunately, Qiu et al. do not report a value for the surface potential of the charged colloids, so that  $C$  cannot be used directly as an input parameter for quantitative comparison with our model. The next best thing is to take the experimentally measured diffusion enhancement at a typical shear rate, e.g.,  $\Delta D_{zz} = 1.4 \cdot 10^{-12} \text{ m}^2/\text{s}$  at  $500 \text{ s}^{-1}$ , and calculate the electrostatic model parameters  $\kappa$  and  $\Phi_a$  that lead to this result, while keeping  $H$  in the regime where  $\Delta D \sim \dot{\gamma}^{0.7}$ . For  $\Phi_a \sim 200 \text{ mV}$  and a ratio of particle radius to Debye length  $\kappa a \sim 0.4$ , our theory matches the diffusion for  $H = 10^4$ , while  $\kappa a$  was estimated to vary between 0.73 (weak interaction) and 0.24 (strong interaction) in the experiments.<sup>[3]</sup> Thus, the theory reproduces the experimentally measured diffusion enhancement and the power law dependence of the latter upon shear rate (seen in simulations) simultaneously for the only available data set. Considering the strong dependence of  $\Delta D$  on the electrostatic parameters (i.e.,  $\Delta D \sim \kappa^{-4.1} e^{0.6\kappa a}$ ) and the imprecision with which these parameters were measured, the theory needs a more stringent experimental test. To this end, diffusion measurements under shear need to be performed on well-characterized systems. The systematic variation of the electrostatic parameters in a low-volume fraction suspension should prove to be an unambiguous experimental test of the theory presented here.

#### ACKNOWLEDGMENTS

VB was supported by the Netherlands Organization for Scientific Research (NWO). AJL acknowledges support by the NSF under award DMR-9870785. We thank D. Pine, S. Ramaswamy, and A. Sood for useful and enjoyable discussion.

## REFERENCES

1. Murray, C.; Grier, D. Colloid crystals. *Am. Sci.* **1995**, *83*, 238.
2. Russel, W.; Saville, D.; Schowalter, W. *Colloidal Dispersions*; Cambridge Univ. Press: Cambridge, 1989.
3. Qiu, X.; Ou-Yang, H.; Pine, D.; Chaikin, P. Self-diffusion of interacting colloids far from equilibrium. *Phys. Rev. Lett.* **1988**, *61*, 2554.
4. Leighton, D.; Acrivos, A. Measurement of shear-induced self-diffusion in concentrated suspensions of spheres. *J. Fluid Mech.* **1987a**, *177*, 109.
5. Breedveld, V.; van den Ende, D.; Tripathi, A.; Acrivos, A. The measurement of the shear-induced particle and fluid tracer diffusivities in concentrated suspensions by a novel method. *J. Fluid Mech.* **1998**, *375*, 297.
6. Foss, D.; Brady, J. Self-diffusion in sheared suspensions by dynamic simulation. *J. Fluid Mech.* **1999**, *401*, 243.
7. Wang, Y.; Mauri, R.; Acrivos, A. The transverse shear-induced liquid and particle tracer diffusivities of a dilute suspensions of spheres undergoing a simple shear flow. *J. Fluid Mech.* **1996**, *327*, 255.
8. Jánosi, I.; Tél, T.; Wolf, D.; Gallas, J. Chaotic particle dynamics in viscous flows: The three-particle Stokeslet problem. *Phys. Rev. E* **1997**, *56*, 2858.
9. Levine, A.; Ramaswamy, S.; Frey, E.; Bruinsma, R. Screened and unscreened phases in sedimenting suspensions. *Phys. Rev. Lett.* **1998**, *81*, 5944.
10. da Cunha, F.; Hinch, E. Shear-induced dispersion in a dilute suspension of rough spheres. *J. Fluid Mech.* **1996**, *309*, 211.
11. Derjaguin, B.; Landau, L. Theory of the stability of strongly charged lyophobic sols and the adhesion of strongly charged particles in solutions of electrolytes. *Acta Physicochimica (USSR)* **1941**, *14*, 633.
12. Verwey, E.; Overbeek, J. *Theory of the Stability of Lyophobic Colloids*; Elsevier: Amsterdam, 1948.
13. Xue, W.; Grest, G. Brownian dynamics simulations for interacting colloids in the presence of a shear flow. *Phys. Rev., A* **1989**, *40*, 1709.
14. Chakrabarti, J.; Sood, A.; Krishnamurthy, H. Brownian-dynamics simulation studies of a charge-stabilized colloidal suspension under shear flow. *Phys. Rev. E* **1994**, *50*, R3326. An examination of their data suggests a power-law dependence of the diffusivities on shear rate with an exponent of  $0.65 \pm 0.05$ .
15. Indrani, A.; Ramaswamy, S. Shear-induced enhancement of self-diffusion in interacting colloidal suspensions. *Phys. Rev., E* **1995**, *52*, 6492.
16. Morris, J.; Brady, J. Self-diffusion in sheared suspensions. *J. Fluid Mech.* **1996**, *312*, 223.
17. van der Vorst, B.; van den Ende, D.; Aelmans, N.; Mellema, J. Shear viscosity of an ordering latex suspension. *Phys. Rev., E* **1997**, *56*, 3119.

Received November 9, 2002

Accepted January 7, 2003

